Pharmacogn. Mag.
A multifaceted peer reviewed journal in the field of Pharmacognosy and Natural Products
www.phcog.com | www.phcog.net

ORIGINAL ARTICLE

Astragaloside Accelerates Fracture Healing via Modulating miR-122/p53 and miR-221/RUNX2 Signaling Pathways

Shaohui Yang, Lingyan Rong, Hongxia Xu, Huihui Liu, Zhenhai Dong

Department of Pharmacy, Wendeng Hospital of Traditional Chinese Orthopedics and Traumatology of Shandong Province, Wendeng, Shandong, China

Submitted: 02-01-2019 Revised: 12-02-2019 Published: 11-02-2020

ABSTRACT

Background: Astragaloside (AS) has been clinically used in the management of fracture, but the underlying mechanism of AS involved in fracture healing is still unknown, so the objective of our study was to explore the above potential mechanism of AS. **Materials and Methods:** 3-(4,5-dimethylthiazol-2-yl)-2,5-diphenyl tetrazolium bromide assay, flow cytometry analysis, real-time polymerase chain reaction, Western blot analysis, computational analysis, luciferase assay, and immunohistochemistry (IHC) were utilized to detect the underlying mechanism of AS involved in fracture healing. **Results:** Cell growth rate, collagen type I, and cell content of osteoblast and MG-63 cell increased while cell apoptosis decreased in a dose-dependent manner compared with controls. MiR-122 and RUNX2 levels showed a stepwise increase while miR-221 and P53 levels showed a stepwise decline as AS concentration increased in osteoblast and MG-63 cells compared with controls. P53 was a virtual target gene of miR-122. Meanwhile, miR-221 directly regulated RUNX2. AS+ group displayed higher messenger RNA (mRNA) levels of miR-122 and RUNX2 than AS– group, while miR-221 and P53 mRNA levels in AS+ group were much lower than AS– group. Results of IHC showed that P53 protein was lowly expressed, while RUNX2 protein was highly expressed in AS+ group compared with AS– group. **Conclusion:** We identified the effects of the regulatory relationship between AS, miR-122, miR-221, P53, and RUNX2 and their effects on the apoptosis of osteoblasts.

Key words: Apoptosis, astragaloside, fracture healing, miR-122, miR-221, p53, RUNX2

SUMMARY

- Astragaloside (AS) has been clinically used in the management of fracture, and it has been found that administration of AS upregulated miR-122 and downregulated miR-221 in patients who received the hip replacement surgery. Furthermore, we found that miR-122 targeted P53 and miR-221 targeted RUNX2, and both of the targets, p53 and RUNX2, work synergically to regulate the apoptosis of the osteoblasts, which have been reported to be functionally involved in the process of fracture healing. In this study, we evaluated the roles of AS in the treatment of fracture and identified the effects of the regulatory relationship between AS, miR-122, miR-221, P53, and RUNX2 and their effects on the apoptosis of osteoblasts.

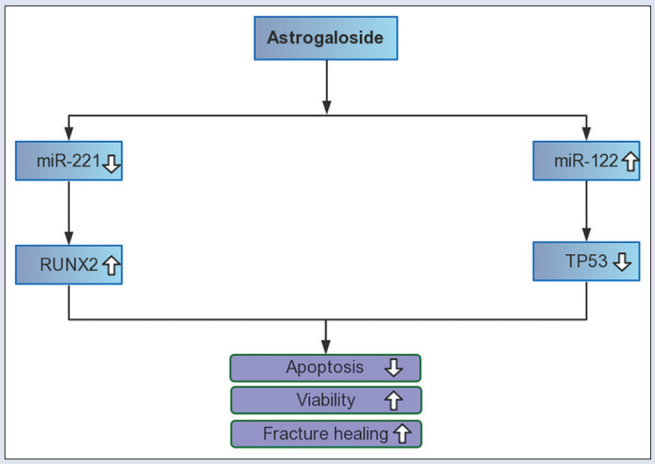

Abbreviations used: AS: Astragaloside; FCM: Flow cytometry; IHC: Immunohistochemistry; AS-IV: Astragaloside IV; miRNA: MicroRNA; HCC: Hepatocellular carcinoma; 3'UTR: 3' untranslated region; DMEM: Dulbecco's modified Eagle's medium; FBS: Fetal bovine serum; MTT assay: 3-(4,5-dimethylthiazol-2-yl)-2,5-diphenyl tetrazolium bromide assay; TBST: Tween 20; HRP: Horseradish peroxidase; SD: Standard deviation; MW: Molecular weight; HDAC: Histone deacetylase.

Correspondence:

Dr. Zhenhai Dong,
1 Fengshan Road, Wendeng 264400,
Shandong, China.
E-mail: orthopedicsoa@yeah.net

DOI: 10.4103/pm.pm_656_18

Access this article online
Website: www.phcog.com
Quick Response Code:

INTRODUCTION

Fracture healing and repair of skeletal tissues are associated with an initial anabolic phase, which are featured by an increased tissue volume originating from the *de novo* stem cell differentiation and recruitment that form vascular and skeletal tissues. In such a way, a cartilaginous callus forms immediately adjacent to the line of fracture. In addition, at the borders of newly formed cartilage tissues around this central region, the periosteum enlarges and the formation of primary bones is initiated.[1,2]

During the process of bone formation and fracture healing, chondrocytes and osteoblasts go through an orderly developmental progression, which ultimately leads to apoptosis.[3,4] During the remodeling of lamellar or osteonal bones, the order of cell events is largely elucidated. However, some past researches did not usually consider controlling the number of osteoblasts through the dual effects of apoptosis and proliferation. The signal transduction pathways involved in the programmed cell death of osteoblasts still remain largely unclear. The withdrawal of estrogen and glucocorticoids can each induce apoptosis in osteocytes and osteoblasts, respectively.[5-7]

AS-IV, 3-O-b-D-xylopyr-anosyl-6-O-b-Dglucopyranosylcyl-cloastragenol, also known as astragaloside (AS) IV, is a major active compound

This is an open access journal, and articles are distributed under the terms of the Creative Commons Attribution-NonCommercial-ShareAlike 4.0 License, which allows others to remix, tweak, and build upon the work non-commercially, as long as appropriate credit is given and the new creations are licensed under the identical terms.

For reprints contact: reprints@medknow.com

Cite this article as: Yang S, Rong L, Xu H, Liu H, Dong Z. Astragaloside accelerates fracture healing via modulating miR-122/p53 and miR-221/RUNX2 signaling pathways. Phcog Mag 2020;16:119-27.

in *Radix Astragali*, a Chinese traditional herbal medicine. According to previous research, AS-IV plays a number of pharmacological roles including antihypertensive, immunoregulatory, anti-inflammatory, antioxidative, and antitumor functions.[8-11] Furthermore, AS-IV also increases the sensibility to antitumor drugs including cisplatin, gefitinib, and fluorouracil.[12-14] Nevertheless, few studies have investigated the pharmacological role of AS-IV in glioma.

MicroRNAs (miRNAs) are short noncoding RNAs of about 22 nucleotides which inhibit the translation of their target messenger RNAs (mRNAs) by binding to them. In such a way, miRNAs exert crucial effects on the regulation of eukaryotic genes, especially during cell apoptosis, differentiation, and proliferation.[15] Generally speaking, the sequence of miRNAs does not need to be perfectly complementary to the 3' untranslated region (3'UTR) of its target mRNA in order to induce mRNA degradation or to suppress its translation.[16] Meanwhile, recent studies have shown that the dysregulation of miRNAs is involved in cardiovascular diseases, such as vascular atherosclerosis, heart failure, and cardiac hypertrophy.[17] In hepatocellular carcinoma (HCC), miR-221 functions as an oncogene and is critical for angiogenesis by inducing the migration and proliferation of endothelial cells through the NOTCH signaling pathway.[18] Moreover, AS-IV was also shown to specifically upregulate miR-122 expression and inhibit miR-221 expression. The results also suggested that the increased miR-122 expression and the inhibited miR-221 expression might contribute to the antiangiogenesis functions of curcumin and AS-IV in HCC.[10]

The well-known transcription factor and tumor-suppressor p53 are sequence specific and directly modulate the expression of a number of its target genes which were involved in the initiation of apoptosis and/or cell cycle arrest.[19,20] In a recent study, RUNX1 was found to function as a scaffold protein to promote the acetylation of p53 as the result of DNA damage, thereby increasing its proapoptotic activity.[21] Interestingly, Blyth *et al.*[22] also demonstrated that RUNX2 could elicit a powerful antiapoptotic signal even when functional p53 was present, suggesting that RUNX2 can neutralize p53. Westendorf *et al.*[23] have demonstrated that RUNX2 inhibited the expression of p21WAF1. Therefore, a functional interaction between RUNX2 and p53 is plausible.

Astragalus (or AS) has been clinically used in the management of fracture, and it has been found that administration of AS upregulated expression of miR-122 and downregulated expression of miR-221 in patients who received the hip replacement surgery.[24,25] Furthermore, we found that miR-122 targeted P53 and miR-221 targeted RUNX2 while both targets, p53 and RUNX2, worked synergically to regulate the apoptosis of the osteoblasts, which have been reported to be functionally involved in the process of fracture healing. In this study, we evaluated the roles of AS in the treatment of fracture and identified the effects of the regulatory relationship between AS, miR-122, miR-221, P53, and RUNX2 and their effects on the apoptosis of osteoblasts.[24,26,27]

MATERIALS AND METHODS

Sample collection

The study was conducted according to the Declaration of Helsinki. Twenty-four participants diagnosed with fracture were recruited for our research consisting of 13 patients who received AS treatment (AS-IV 2.5 mg/kg/day for 2 weeks) and 11 patients who did not receive AS treatment. To be specific, 7 male patients aging from 45 to 60 years and 6 female patients aging from 39 to 55 years were recruited as fracture patients who received AS treatment. Moreover, for the fracture patients who did not receive AS treatment, the sex ratio was 6:5 as males to females, aging from 43 to 58 years and 42–61 years, respectively. All female patients included do not suffer from menopausal. The diagnosis of fracture was confirmed by X-ray film, and those who were diagnosed with other pathological conditions of bone such as osteosarcoma, giant cell tumor, or osteoporosis or osteopenia were excluded from the present study. The patients have already signed informed consent for participation in the study. The institution's Ethics and Research Committees of China Medical University had already agreed with this study.

RNA isolation and real-time polymerase chain reaction

TRIzol reagent (Life Technologies Corporation, Carlsbad, CA, US) was utilized to isolate total RNA from osteoblast and SG-63 cells or tissue samples following manufacturer's guideline. Sprint Power Script Primed Single Shots Kit (Clontech, Mountain View, CA, USA) was utilized to synthesize first-strand cDNA from RNA extracted. Titanium Taq DNA polymerase (Clontech, Mountain View, CA, US) was utilized to amplify cDNAs, and the reaction was carried out as follows: 35 cycles of 94°C for 30 s, 60°C for 30 s, and 68°C for 60 s. 2% agarose gel electrophoresis was utilized to fractionate all polymerase chain reaction (PCR) products, and then, ethidium bromide was utilized to visualize all PCR products. To perform real-time PCR analysis to analyze relative expressions of miR-221, miR-122, RUNX2, and P53, 2× SYBR Green PCR Master Mix (Applied Biosystems, Foster City, CA, USA) was utilized to perform real-time quantitative PCR using ABI 7300 Real-Time PCR System (Applied Biosystems). U6 or GAPDH was used as an internal control to normalize expressions of miR-221 and miR-122 or RUNX2 and P53, respectively. Comparative CT method was utilized to calculate relative expressions of miR-221, miR-122, RUNX2, and P53. Each reaction was run three times.

Cell culture and treatment

Dulbecco's modified Eagle's medium (Thermo Fisher Scientific, Waltham, MA, US) containing 100 μg/mL streptomycin, 100 U/mL penicillin (Thermo Fisher Scientific, Waltham, MA, US), and 10% fetal bovine serum (Harlan Sera-Lab, UK) was utilized to incubate osteoblast and SG-63 cells in a 5% CO_2/95% air atmosphere at 37°C. When osteoblast and SG-63 cells were grown to 70% confluent, cells were treated with 1, 10, and 100 nM AS and then transfected with miR-221 or miR-122 mimic using Lipofectamine 2000 (Thermo Fisher Scientific, Waltham, MA, US) following standard protocol. 10 mg/mL puromycin was utilized to select transfected cells. Each experiment was performed in triplicate.

Cell proliferation assay

Osteoblast and SG-63 cells transfected with miR-221 or miR-122 mimic were grown into 24-well plates with a final density of 5×10^3 cells per well. (3-(4,5-dimethylthiazol-2-yl)-2,5-diphenyl tetrazolium bromide [MTT]) assay was utilized to analyze cell viability. In brief, MTT (0.25 mg/mL) was added into each well and followed by incubation for another 4 h at 37°C and 150 mL was added into each well. An enzyme-linked immunosorbent assay reader (Thermo Scientific, Waltham, Massachusetts, USA) was utilized to examine cell proliferation based on absorbance at 490 nm. All reactions were repeated three times.

Luciferase assay

The fragment of P53 or RUNX2 3'UTR with binding site of miR-122 or miR-221 was amplified by PCR, and then, PCR products were inserted into firefly luciferase reporter. The binding site of miR-122 or miR-221 located on P53 or RUNX2 3'UTR was mutated using QuikChange mutagenesis kit (Stratagene, La Jolla, CA, USA) based on manufacturer's protocol. When the osteoblast and SG-63 cells were grown to 80% confluence, Lipofectamine 2000 (Invitrogen, Carlsbad, CA, USA) was utilized to performed transfection, and cells were transfected miR-122 or miR-221 mimics and constructs containing wild-type P53 or RUNX2 3'UTR

and mutant P53 or RUNX2 3'UTR following manufacturer instruction. 48 h after transfection, osteoblast and SG-63 cells were harvested. Dual-Luciferase Reporter Assay System (Promega, Madison, WI, USA) was utilized to detect the luciferase activity of Renilla and firefly based on the standard instruction by the supplier. All tests were run in triplicate.

Western blot analysis

Buffer containing 0.5% sodium deoxycholate, 1% Triton X-100, 50 mM Tris (pH 7.5), 0.5 mM dithiothreitol, 2 mM EDTA, 1 mM PMSF, 150 mM NaCl, phosphatase inhibitor (Sigma-Aldrich, St. Louis, MO, USA), and protease inhibitor cocktail (Sigma-Aldrich, St. Louis, MO, US) was utilized to lyse PTENCE cells after transfection. 10% sodium dodecyl sulfate–polyacrylamide gel electrophoresis was utilized to separate protein and electrotransferred to the nitrocellulose membranes (GE Healthcare, Little Chalfont, UK). A buffer containing 5% nonfat milk in phosphate-buffered saline with 0.05% Tween 20 (TBST) was used to block the membranes for 90 min. TBST was utilized to wash the membrane three times. Primary goat antibodies against P53 or RUNX2 diluted 1:5000 (Santa Cruz Biotechnology, Santa Cruz, CA, USA) or against β-actin diluted 1:8000 (Abcam, Cambridge, MA, USA) were utilized to treat the membrane at room temperature for 120 min, and then, TBST was utilized to wash the membrane three times. Horseradish peroxidase (HRP)-labeled anti-goat secondary antibodies at a dilution of 1:12000 (BOSTER, Wuhan, China) were utilized to maintain the membrane at 25°C for 2 h. TBST was utilized to wash the membrane three times. Immobilon Western Chemiluminescent HRP Substrate (Millipore, Billerica, MA, USA) was utilized to detect the signals. ImageJ1.37 software (NIH, Bethesda, MD, USA) was utilized to perform densitometric quantitation. Three independent experiments were carried out.

Apoptosis analysis

Annexin V-FITC and 7-aminoactinomycin D staining kit (Beckman Coulter, Inc., Fullerton, CA) was utilized to measure cell apoptosis based on manufacturer's recommendation. Ice-cold PBS was utilized to wash osteoblast and SG-63 cells; 20 mL of 7-aminoactinomycin D viability dye and 10 mL Annexin V-FITC solution were utilized to incubate cells in darkness; then, 400 mL Annexin V binding buffer was utilized to treat cell. Flow cytometry (Beckman Coulter, Inc., Fullerton, CA) was utilized to analyze cell apoptosis within 30 min. Three independent tests were repeated.

Immunohistochemistry

Four percent paraformaldehyde was utilized to fix tissue samples, and xylene and ethanol were utilized to deparaffinize tissue samples. 10 mM citrate buffer (pH 6.0) was utilized to perform antigen retrieval, and 10% normal goat serum was utilized to block the sections for 30 min. TBST was utilized to wash the membrane three times. Primary goat antibodies against P53 or RUNX2 diluted 1:200 (Santa Cruz Biotechnology, Santa Cruz, CA, USA) were utilized to treat the sections at 4°C for 12 h, and then, TBST was utilized to wash the sections three times. HRP-labeled anti-goat secondary antibodies at a dilution of 1:1000 (BOSTER, Wuhan, China) were utilized to maintain the membrane at 25°C for 2 h, followed by counterstained with methyl green-pyronin stain solution; a light microscope was utilized to examine the sections at a magnification of ×100.

Statistical analysis

Each test was presented as mean ± standard deviation; SPSS version 20.0 statistical soft (SPSS Inc., Chicago, IL, USA) was utilized to perform statistical analysis. Chi-square test and Student's *t*-test were utilized to perform comparisons between two groups while one-way ANOVA was performed to compare differences among more than two groups. $P < 0.05$ was considered as statistically significant.

RESULTS

Astragaloside altered cell proliferation and apoptosis, alkaline phosphatase, collagen type I, and content of cell

Before measuring the proliferation, apoptosis, alkaline phosphatase (ALP), collagen type I, and content of osteoblast and MG-63 cells, the cells were treated with different doses of AS (1, 10, and 100 nM). As shown in Figures 1 and 2, AS dose dependently increased cell growth rate [Figure 1a and 2a] of osteoblast [Figure 1] and MG-63 [Figure 2] cells, ALP [Figure 1c and 2c] and collagen type I [Figure 1d and 2d] in osteoblast [Figure 1] and MG-63 [Figure 2] cells, and content [Figure 1e and 2e] of osteoblast [Figure 1] and MG-63 [Figure 2] cells compared with controls, while AS suppressed cell apoptosis [Figure 1b and 2b] of osteoblast under a dose-dependent manner in comparison with the control groups.

Determination effect of astragaloside on miR-122, miR-221, p53, and RUNX2 levels

Meanwhile, after treated with different doses of AS (1, 10, and 100 nM), real-time PCR and Western blot analysis were performed to examine expression levels of miR-122, miR-221, p53, and RUNX2 in osteoblast and MG-63 cells. As shown in Figure 3 and 4, miR-122 mRNA [Figure 3a and 4a], RUNX2 mRNA [Figure 3d and 4d], and protein [Figure 3e and 4e] levels in osteoblast [Figure 3] and MG-63 [Figure 4] cells dose dependently increased subsequent to treat with stepwise increase dose of AS compared to those in corresponding controls. MiR-221 mRNA [Figure 3b and 4b], p53 mRNA [Figure 3c and 4c], and protein [Figure 3e and 4e] levels showed a stepwise decline as the concentration of AS increased in osteoblast [Figure 3] and MG-63 [Figure 4] cells when compared with the negative controls, validating that AS upregulated the levels of miR-221 and RUNX2, while downregulating miR-122 and P53 expressions.

P53 was a candidate target gene of miR-122

Online publicly available algorithms (mirdb.org) were utilized to explore the mechanism underlying the effects of AS upon fracture healing mediated by miR-122. Accordingly, P53 was identified as a candidate target gene of miR-122 with a complementary binding site of miR-122 on P53 3'UTR [Figure 5a]. Luciferase assay was further conducted to confirm the interaction between miR-122 and P53. Constructs containing wild-type or mutant P53 3'UTR were generated and cotransfected with miR-122 mimic into osteoblast [Figure 5a] and MG-63 [Figure 5b] cells, presenting evident decrease in luciferase activity of wild-type P53 3'UTR but not that of mutant P53 3'UTR of osteoblast [Figure 5b] and MG-63 [Figure 5c] cells transfected with miR-122 mimic, thus suggesting that miR-122 directly targeted and inhibited P53 expression.

MiR-221 directly regulated RUNX2

Online publicly available algorithms (mirdb.org) also identified that RUNX2 was a candidate target gene of miR-221 with a binding site of miR-122 [Figure 6a]. Luciferase assay was performed to further confirm the interaction between miR-221 and RUNX2. As shown in Figure 6, luciferase activity of wild-type RUNX2 3'UTR in osteoblast [Figure 6b] and MG-63 [Figure 6c] cells transfected with miR-122 mimic was obviously downregulated compared with controls, while luciferase

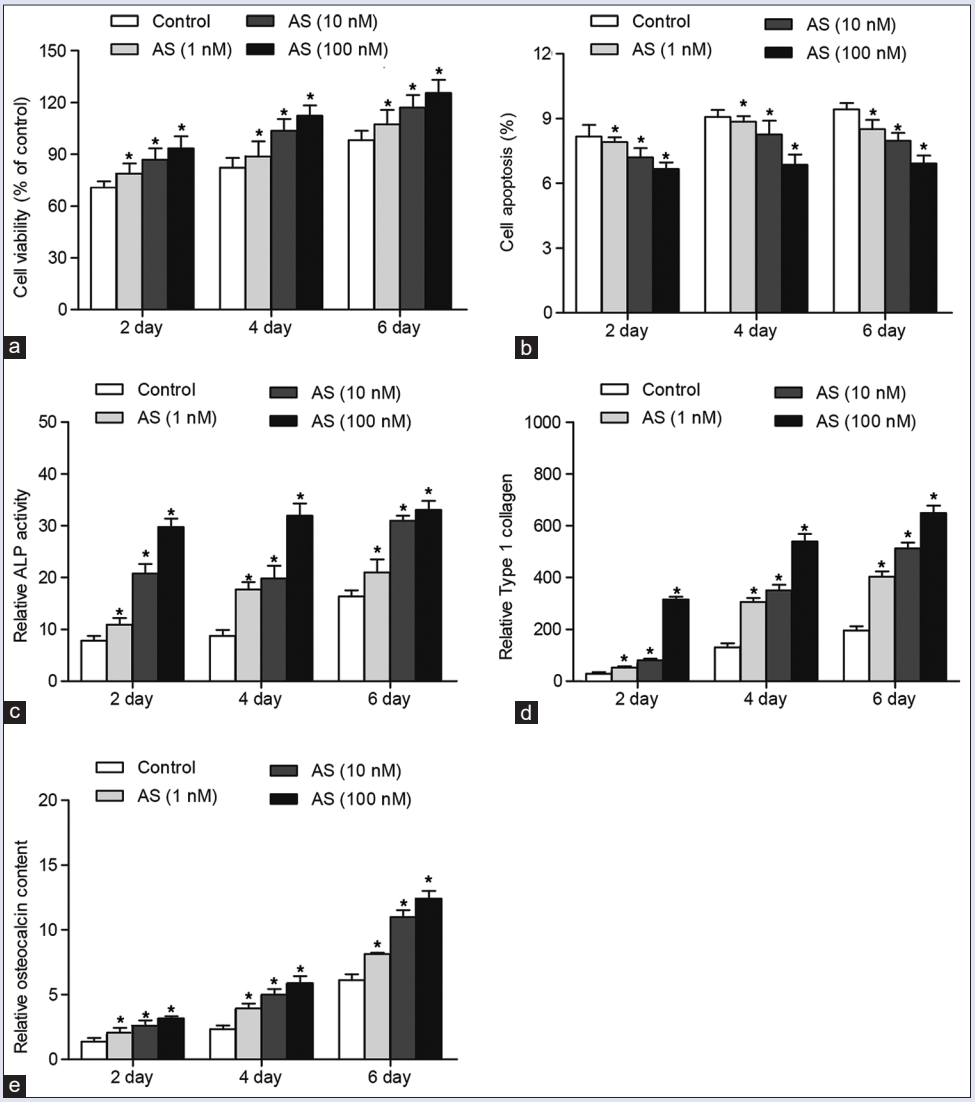

Figure 1: Alternation cell proliferation and apoptosis, alkaline phosphatase, collagen type I, and content of osteoblast by AS treatment (*$P < 0.05$, vs. control group). (a) Astragaloside dose dependently upregulated cell viability compared with controls. (b) AS dose dependently downregulated cell apoptosis compared with controls. (c) Alkaline phosphatase activity showed a stepwise increase as the concentration of astragaloside treatment increased when compared with controls. (d) Collagen type I was dose dependently upregulated in cell treated with astragaloside. (e) Content of osteoblast treated with various dose of as showed a stepwise increase compared with controls

activity of mutant RUNX2 3'UTR was comparable with controls, indicating that RUNX2 was a virtual target gene of miR-221.

Differential levels of MiR-122, miR-221, p53, and RUNX2 between AS+ and AS– groups

Twenty-four patients diagnosed with fracture were recruited, and 13 fracture patients received AS treatment (AS+ group) and 11 fracture patients did not receive AS treatment (AS– group). Levels of miR-122, miR-221, p53, and RUNX2 between AS+ and AS– groups were determined by performing real-time PCR and immunohistochemistry. As shown in Figure 7 and 8, miR-122 mRNA [Figure 7a], RUNX2 mRNA [Figure 7d], and protein [Figure 8b] levels in AS+ group were much higher than AS– group, while miR-221 mRNA [Figure 7b], P53 mRNA [Figure 7c], and protein [Figure 8a] levels in AS+ group were much lower than AS– group.

DISCUSSION

AS-IV, 3-0-beta-Dxylopyranosyl-6-0-beta-D-glucopyranos-ylcyc loastragenol, a major active component in *Astragalus membranaceus*, is a purified saponin with a small molecular weight (MW 784). Pharmacological investigations have shown that AS-IV exerts a number of protective effects, including anti-inflammation, antihypertension, antinociception, positive inotropic action, antiviral, and anti-infarction functions.[8,9,28-31] It was also shown that AS treatment could improve the circulation of the wound or fracture and possibly re-open the blocked vessels.[28-30] AS was also demonstrated to induce the differentiation of osteoblasts by improving the excretion and mineralization of ALP as well as the expression of osteoblast marker genes. In addition, it was also reported that AS-I induced the differentiation of osteoblasts via the Wnt-catenin signaling pathway, which in turn activated the BMP signaling and downregulated the RANK signaling. Nevertheless, it is necessary to carry out further studies in order to clarify the functions of

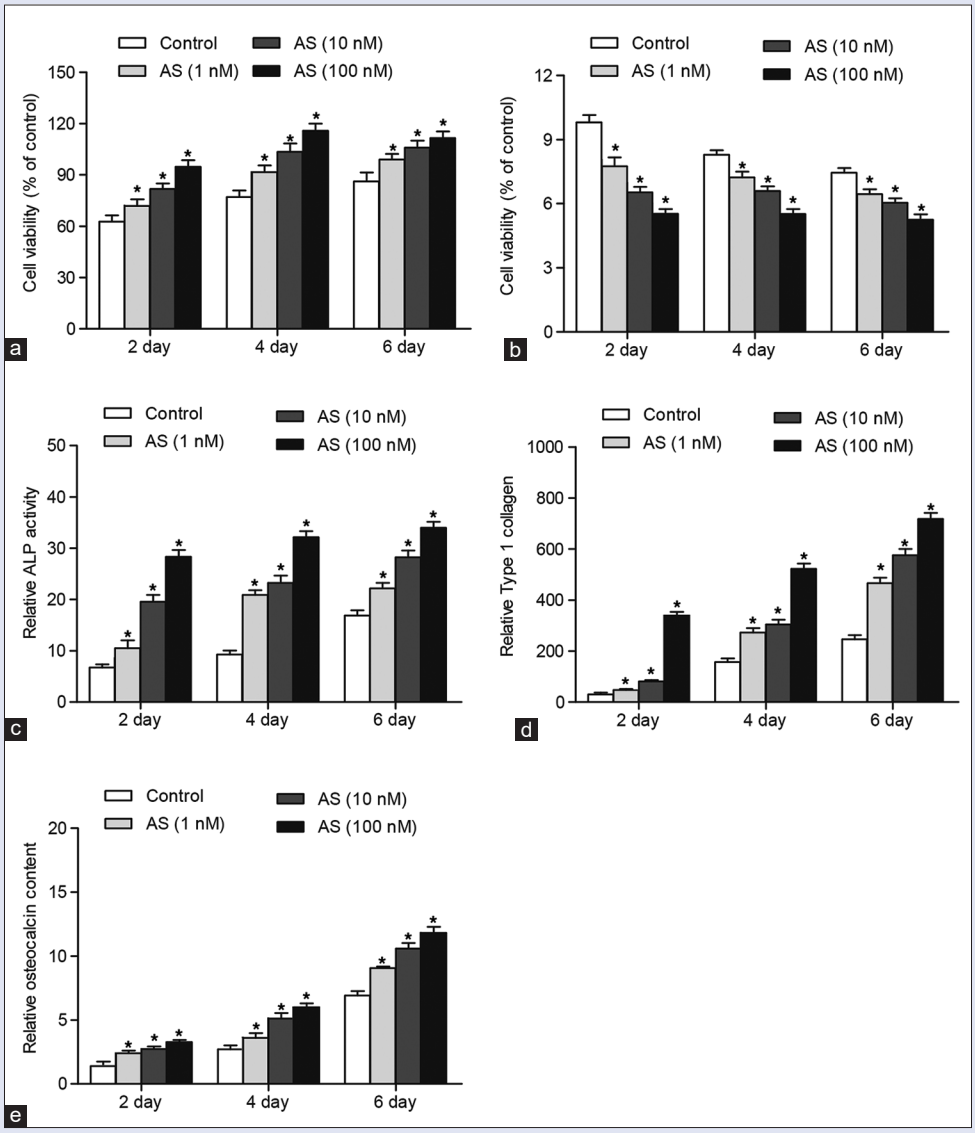

Figure 2: Alternation cell proliferation and apoptosis, alkaline phosphatase, collagen type I, and content of MG-63 by AS treatment (*$P < 0.05$, vs. control group). (a) Astragaloside dose dependently upregulated cell viability compared with controls. (b) Astragaloside dose dependently downregulated cell apoptosis compared with controls. (c) Alkaline phosphatase activity showed a stepwise increase as the concentration of astragaloside treatment increased when compared with controls. (d) Collagen type I was dose dependently upregulated in cell treated with astragaloside. (e) Content of MG-63 treated with various doses of astragaloside showed a stepwise increase compared with controls

BMP and RANK signaling pathways in the differentiation of osteoblasts and osteoclasts.[25] In this study, we detected cell proliferation and apoptosis, ALP, collagen type I, and content of osteoblast and MG-63 cells treated with different doses of AS and found that cell viability, collagen type I, and cell content were dose dependently upregulated than controls, while cell apoptosis was downregulated under a dose-dependent manner compared with controls.

It was found that AS-IV could promote angiogenesis after AMI in rats. In addition, the results showed that AS-IV and miR-221 mimics can both activate angiogenesis, whereas the inhibitors of miR-221 suppressed the AS-IV-dependent angiogenesis in EA-hy926 cells. AS-IV also increased the expression of VEGF and AKT by regulating miR-22,1 and the effect of AS-IV was abolished after treating the cells with miR-221 inhibitors. Therefore, it is proposed that the induction effect of AS-IV on angiogenesis is attributed to the activation of the VEGF/AKT signaling pathway mediated by miR-221.[32] MiR-122 has been shown to regulate the p53/Akt signaling pathway as well as the apoptosis induced by chemotherapy in cutaneous T-cell lymphoma.[33] By regulating the expression of its target gene cyclin-G1, miR-122 also affects the transcriptional activity and stability of p53 proteins and reduces the invasiveness of HCC-derived cell lines.[34] Furthermore, the overexpression of miR-122 induces doxorubicin-dependent apoptosis of HCC-derived cell lines. Nevertheless, the exact mechanism underlying the induction of p53-dependent apoptosis by the overexpression of miR-122 in cholangiocarcinoma cells (possibly via cyclin-G1) was not studied in this research and hence remains unclear.

By transfecting human adipose-derived mesenchymal stem cells (hADMSCs) with miR-221 mimics, the degree of osteogenic differentiation was elevated, although the degree of adipogenic differentiation was significantly inhibited by miR-221 mimics. Histone deacetylase 6 (HDAC6) is a corepressor of RUNX2 and has been identified as a miR-221 target. In addition, the overexpression of

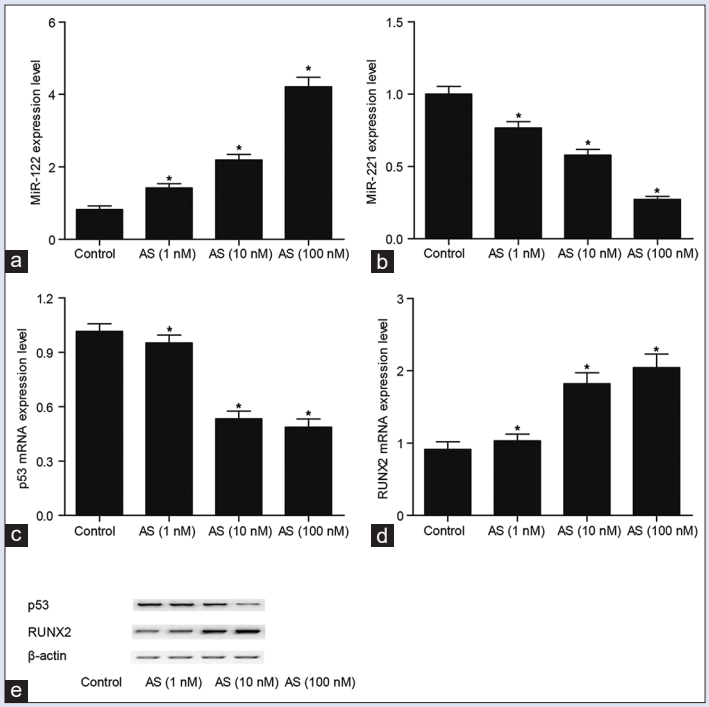

Figure 3: Determination effect of AS on miR-122, miR-221, p53, and RUNX2 levels in osteoblast using real-time polymerase chain reaction and Western blot analysis (*$P < 0.05$, vs. control group). (a) Astragaloside dose dependently enhanced miR-122 expression compared with controls. (b) Treating with AS dose dependently reduced miR-221 messenger RNA level compared with controls. (c) P53 messenger RNA level showed a stepwise decline as the concentration of astragaloside treatment increased when compared with controls. (d) RUNX2 messenger RNA in cells treated with different dose of astragaloside displayed a stepwise increase compared with controls. (e) AS treatment dose dependently upregulated P53 and RUNX2 protein levels compared with controls

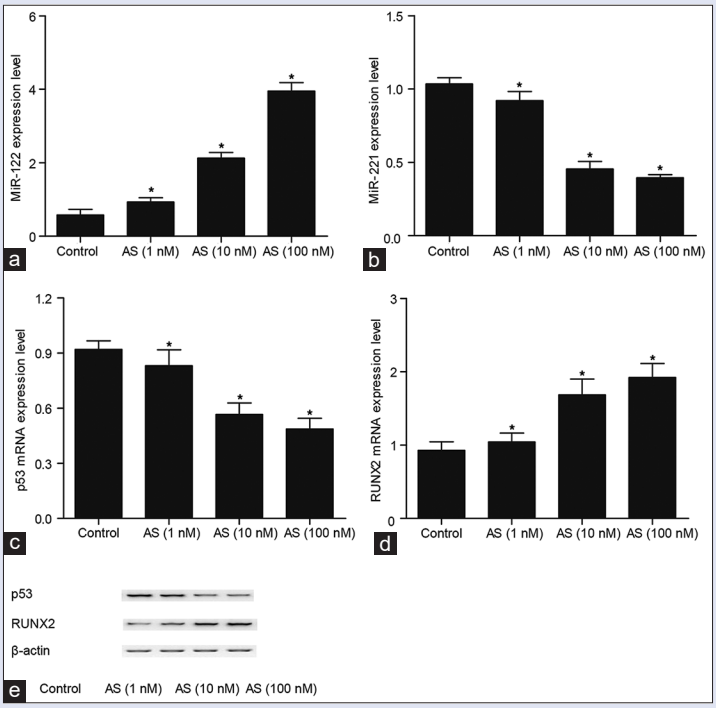

Figure 4: Determination effect of AS on miR-122, miR-221, p53, and RUNX2 levels in MG-63 using real-time polymerase chain reaction and Western blot analysis (*$P < 0.05$, vs. control group). (a) Astragaloside dose dependently enhanced miR-122 expression compared with controls. (b) Treating with astragaloside dose dependently reduced miR-221 messenger RNA level compared with controls. (c) P53 messenger RNA level showed a stepwise decline as the concentration of astragaloside treatment increased when compared with controls. (d) RUNX2 messenger RNA in cells treated with different dose of astragaloside displayed a stepwise increase compared with controls. (e) Astragaloside treatment dose dependently upregulated P53 and RUNX2 protein levels compared with controls

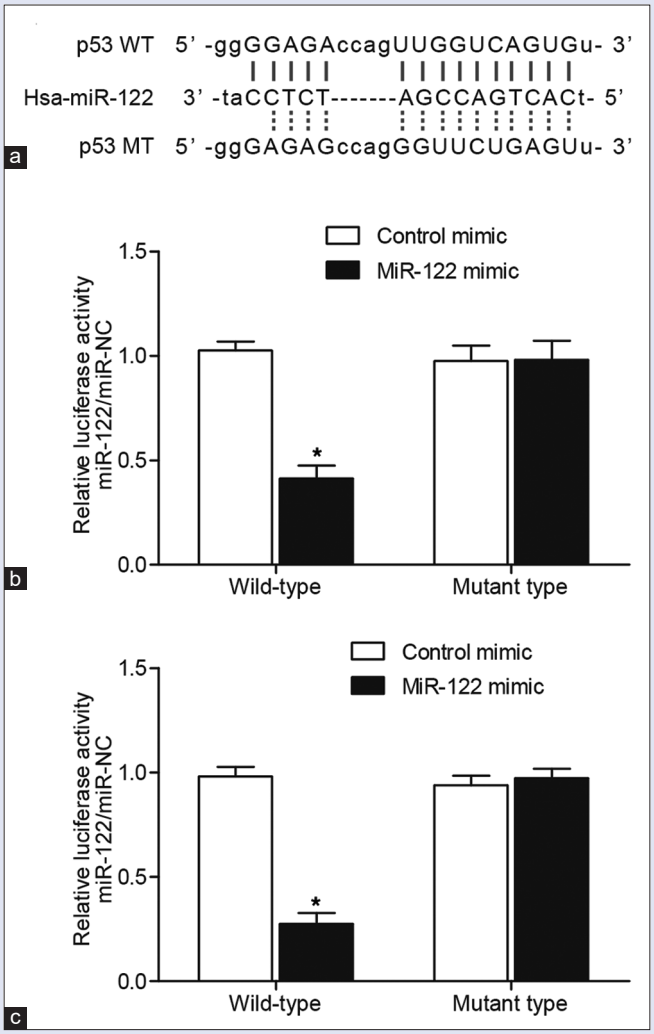

Figure 5: P53 was a candidate target gene of miR-122 (*$P < 0.05$, vs. control group). (a) P53 was identified as the candidate target gene of miR-122 in osteoblast with the "seed sequence" in the 3′ untranslated region of P53. (b) Luciferase activity of wild-type P53 3′ untranslated region but not that of mutant P53 3′ untranslated region in osteoblast was reduced by transfecting with miR-122 mimic. (c) MG-63 cells transfected with miR-122 mimic exhibited a lower luciferase activity of wild-type P53 3′ untranslated region

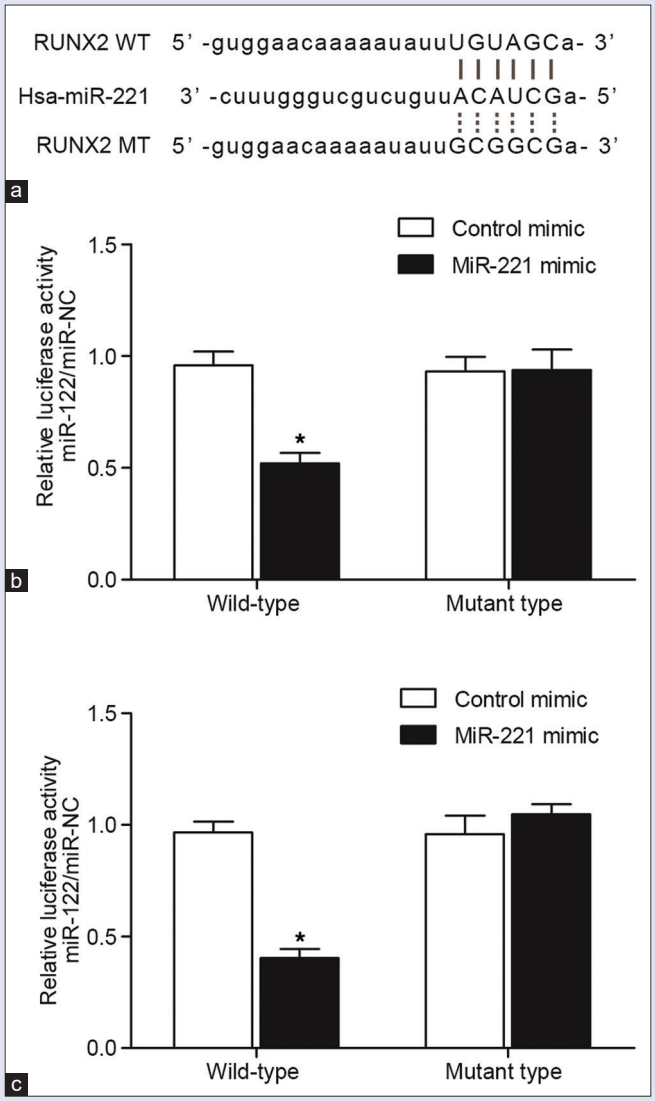

Figure 6: MiR-221 directly regulated RUNX2 (*$P < 0.05$, vs. control group). (a) The 3′-UTR of RUNX2 is targeted by miR-221 with potential "hit" in the 3′ untranslated region of RUNX2. (b) Luciferase activity of wild-type RUNX2 3′ untranslated region but not that of mutant RUNX2 3′ untranslated region in osteoblast was reduced by transfecting with miR-221 mimic. (c) MG-63 cells transfected with miR-221 mimic exhibited a lower luciferase activity of wild-type RUNX2 3′ untranslated region

miR-221 as well as the inhibition of HDAC6 induced the formation of osteoblasts while not affecting the expression levels of RUNX2.[22] These results suggested that HDAC6 might control osteogenic differentiation by interacting with RUNX2 proteins directly to inhibit the expression of osteogenic-related genes. Such mechanism may contribute to the regulation of osteogenic differentiation by miR-22.[35] Based on the literature and the data of this study, administration of AS could alter the expression of miR-122 and miR-221. Using the *in silico* analysis and luciferase reporter system, we identified that P53 was a direct target of miR-122 and RUNX2 was a direct target of miR-221.

The p53 gene encodes an important tumor suppressor and is highly conserved among vertebrate species.[36-38] In more than half of all human tumors, p53 is either missing or mutated and its inactivation is considered as an important step during carcinogenesis.[39] Wild-type p53 can arrest the growth of cells.[39-42] RUNX2 has two isoforms (type I RUNX2 starts with a sequence MRIPV and type II RUNX2 starts with a sequence MASNS), which are associated with different N-termini and are controlled by different promoters.[43] Both of these RUNX2 isoforms are expressed in osteoblasts and chondrocytes, although the expression of type II RUNX2 is predominant in osteoblasts.[44] The two RUNX2 isoforms exert similar effects, although they are different in terms of Cbfb dependency involving this essential cotranscription factor of RUNX2.[45] During the development of skeletal tissues, both of the two RUNX2 isoforms are poorly expressed in proliferating chondrocytes, and the level of expression is gradually increased with the differentiation of chondrocytes. In maturating chondrocytes from prehypertrophic to terminal hypertrophic stages, the expression of both RUNX2 isoforms is high.[46] In this study, we enrolled 24 fracture patients consisting of 13 fracture patients who received AS treatment and 11 fracture patients who did not receive AS treatment and found that AS+ group exhibited higher levels of miR-122 and RUNX2 than AS− group, while miR-221

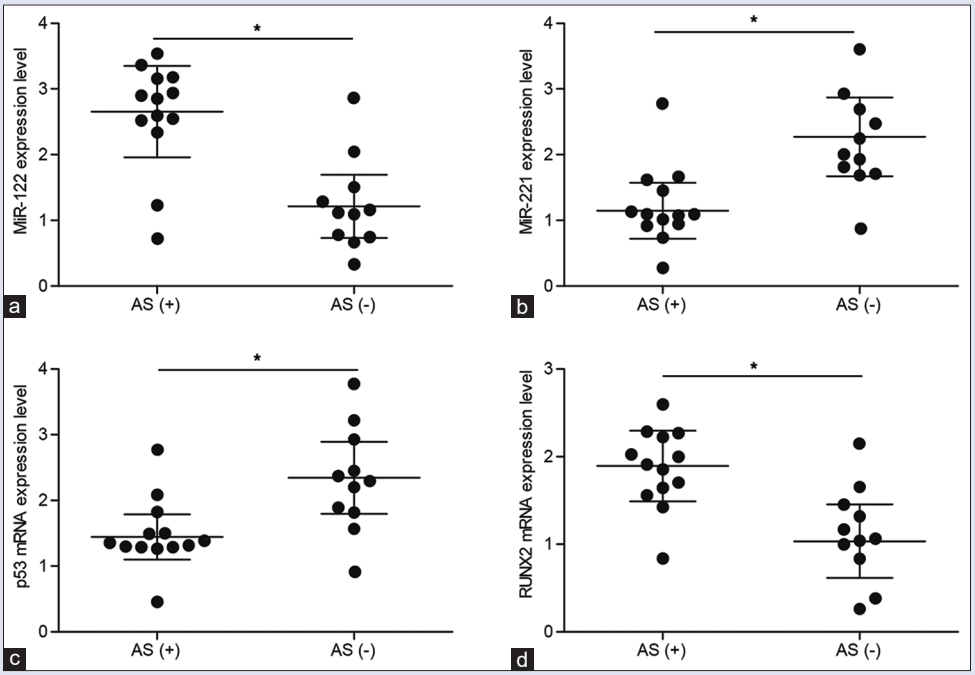

Figure 7: Differential messenger RNA levels of MiR-122, miR-221, p53, and RUNX2 between AS+ and AS− groups (*$P < 0.05$, vs. AS− group). (a) miR-122 level in AS+ group was much higher than AS− group. (b) AS+ group displayed a lower level of miR-221 compared with AS− group. (c) P53 messenger RNA level was much lower in AS+ group than AS− group. (d) RUNX2 messenger RNA was highly expressed in AS+ group compared with AS− group

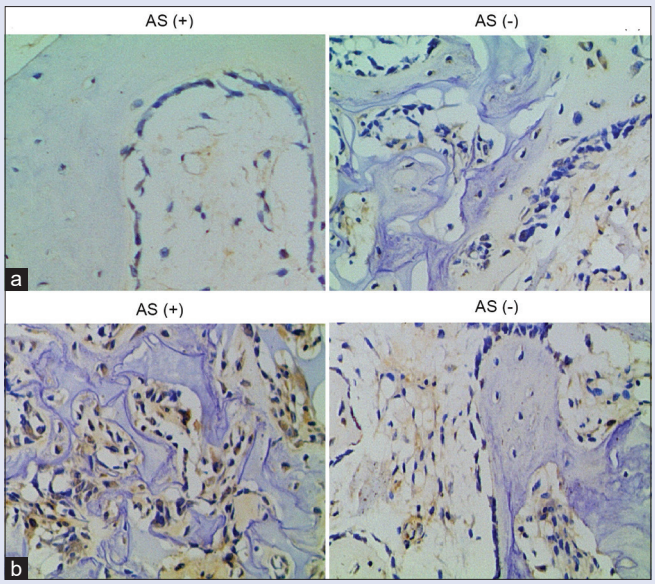

Figure 8: Differential protein levels of p53 and RUNX2 between AS+ and AS− groups presented at the magnification of ×100. (a) P53 protein level was much lower in AS+ group than AS− group. (b) RUNX2 protein was highly expressed in AS+ group compared with AS− group

and P53 mRNA levels in AS+ group were much lower than AS− group.

Recently, it was found that RUNX3 and RUNX1 increase the DNA damage-induced proapoptotic activity of p53 by inducing the ATM-dependent phosphorylation of p53 and the p300-dependent acetylation of p53, respectively.[21,47] These results led to an investigation on whether RUNX2 also participates in the p53-dependent response to DNA damages. In this study, it has been demonstrated that the elevated expression of RUNX2 inhibited the transcriptional activation of its target genes that were dependent on p53. In addition, the inhibition of RUNX2 expression increased the Adriamycin (ADR)-dependent proapoptotic activity of p53, which further stimulated the expression of its target genes following ADR exposure. These results suggested that, in contrary to RUNX1 and RUNX3, RUNX2 plays an inhibitory role during the regulation of p53.

In addition, AS-I has also been reported to function similarly as AS-IV to induce the differentiation of osteoblasts by activating BMP signaling pathway,[24,26] and further study about the therapeutic effect of AS-IV in the treatment of fracture is also warranted.

CONCLUSION

AS has been clinically used in the management of fracture, and it has been found that administration of AS upregulated miR-122 and downregulated miR-221 in patients who received the hip replacement surgery. Furthermore, we found that miR-122 targeted P53 and miR-221 targeted RUNX2, and both of the targets, p53 and RUNX2, work synergically to regulate the apoptosis of the osteoblasts, which have been reported to be functionally involved in the process of fracture healing. In this study, we evaluated the roles of AS in the treatment of fracture and identified the effects of the regulatory relationship between AS, miR-122, miR-221, P53, and RUNX2 and their effects on the apoptosis of osteoblasts.

Financial support and sponsorship

Nil.

Conflicts of interest

There are no conflicts of interest.

REFERENCES

1. Phillips AM. Overview of the fracture healing cascade. Injury 2005;36 Suppl 3:S5-7.
2. Claes L, Recknagel S, Ignatius A. Fracture healing under healthy and inflammatory conditions. Nat Rev Rheumatol 2012;8:133-43.
3. Lynch MP, Capparelli C, Stein JL, Stein GS, Lian JB. Apoptosis during bone-like tissue development *in vitro*. J Cell Biochem 1998;68:31-49.
4. Tomkinson A, Reeve J, Shaw RW, Noble BS. The death of osteocytes via apoptosis accompanies estrogen withdrawal in human bone. J Clin Endocrinol Metab 1997;82:3128-35.
5. Landry P, Sadasivan K, Marino A, Albright J. Apoptosis is coordinately regulated with osteoblast formation during bone healing. Tissue Cell 1997;29:413-9.
6. Tomkinson A, Gevers EF, Wit JM, Reeve J, Noble BS. The role of estrogen in the control of rat osteocyte apoptosis. J Bone Miner Res 1998;13:1243-50.
7. Weinstein RS, Jilka RL, Parfitt AM, Manolagas SC. Inhibition of osteoblastogenesis and promotion of apoptosis of osteoblasts and osteocytes by glucocorticoids. Potential mechanisms of their deleterious effects on bone. J Clin Invest 1998;102:274-82.
8. Zhang WD, Zhang C, Liu RH, Li HL, Zhang JT, Mao C, *et al.* Preclinical pharmacokinetics and tissue distribution of a natural cardioprotective agent astragaloside IV in rats and dogs. Life Sci 2006;79:808-15.
9. Zhang WJ, Hufnagl P, Binder BR, Wojta J. Antiinflammatory activity of astragaloside IV is mediated by inhibition of NF-kappaB activation and adhesion molecule expression. Thromb Haemost 2003;90:904-14.
10. Zhang S, Tang D, Zang W, Yin G, Dai J, Sun YU, *et al.* Synergistic inhibitory effect of traditional Chinese medicine astragaloside IV and curcumin on tumor growth and angiogenesis in an orthotopic nude-mouse model of human hepatocellular carcinoma. Anticancer Res 2017;37:465-73.
11. Jiang K, Lu Q, Li Q, Ji Y, Chen W, Xue X, *et al.* Astragaloside IV inhibits breast cancer cell invasion by suppressing vav3 mediated rac1/MAPK signaling. Int Immunopharmacol 2017;42:195-202.
12. Xie T, Li Y, Li SL, Luo HF. Astragaloside IV enhances cisplatin chemosensitivity in human colorectal cancer via regulating NOTCH3. Oncol Res 2016;24:447-53.
13. Wang M, Huang C, Su Y, Yang C, Xia Q, Xu DJ, *et al.* Astragaloside II sensitizes human hepatocellular carcinoma cells to 5-fluorouracil via suppression of autophagy. J Pharm Pharmacol 2017;69:743-52.
14. Dai PC, Liu DL, Zhang L, Ye J, Wang Q, Zhang HW, *et al.* Astragaloside IV sensitizes non-small cell lung cancer cells to gefitinib potentially via regulation of SIRT6. Tumour Biol 2017;39. doi: 10.1177/1010428317697555.
15. Sempere LF, Freemantle S, Pitha-Rowe I, Moss E, Dmitrovsky E, Ambros V, *et al.* Expression profiling of mammalian microRNAs uncovers a subset of brain-expressed microRNAs with possible roles in murine and human neuronal differentiation. Genome Biol 2004;5:R13.
16. Ambros V. The functions of animal microRNAs. Nature 2004;431:350-5.
17. Pan ZW, Lu YJ, Yang BF. MicroRNAs: A novel class of potential therapeutic targets for cardiovascular diseases. Acta Pharmacol Sin 2010;31:1-9.
18. Nicoli S, Knyphausen CP, Zhu LJ, Lakshmanan A, Lawson ND. MiR-221 is required for endothelial tip cell behaviors during vascular development. Dev Cell 2012;22:418-29.
19. Vousden KH, Lu X. Live or let die: The cell's response to p53. Nat Rev Cancer 2002;2:594-604.
20. Oren M. Decision making by p53: Life, death and cancer. Cell Death Differ 2003;10:431-42.
21. Wu D, Ozaki T, Yoshihara Y, Kubo N, Nakagawara A. Runt-related transcription factor 1 (RUNX1) stimulates tumor suppressor p53 protein in response to DNA damage through complex formation and acetylation. J Biol Chem 2013;288:1353-64.
22. Blyth K, Vaillant F, Hanlon L, Mackay N, Bell M, Jenkins A, *et al.* RUNX2 and MYC Collaborate in Lymphoma Development by Suppressing Apoptotic and Growth Arrest Pathways *In vivo*. Cancer Res 2006;66:2195-201.
23. Westendorf JJ, Zaidi SK, Cascino JE, Kahler R, van Wijnen AJ, Lian JB, *et al.* RUNX2 (Cbfa1, AML-3) interacts with histone deacetylase 6 and represses the p21(CIP1/WAF1) promoter. Mol Cell Biol 2002;22:7982-92.
24. Zhang Y, Gao Y, Cai L, Li F, Lou Y, Xu N, *et al.* MicroRNA-221 is involved in the regulation of osteoporosis through regulates RUNX2 protein expression and osteoblast differentiation. Am J Transl Res 2017;9:126-35.
25. Cheng X, Wei B, Sun L, Hu X, Liang J, Chen Y, *et al.* Astragaloside I stimulates osteoblast differentiation through the wnt/β-catenin signaling pathway. Phytother Res 2016;30:1680-8.
26. Wu C, Zhang J, Cao X, Yang Q, Xia D. Effect of mir-122 on human cholangiocarcinoma proliferation, invasion, and apoptosis through P53 expression. Med Sci Monit 2016;22:2685-90.
27. Pereira BP, Zhou Y, Gupta A, Leong DT, Aung KZ, Ling L, *et al.* Runx2, p53, and pRB status as diagnostic parameters for deregulation of osteoblast growth and differentiation in a new pre-chemotherapeutic osteosarcoma cell line (OS1). J Cell Physiol 2009;221:778-88.
28. Yang Q, Lu JT, Zhou AW, Wang B, He GW, Chen MZ, *et al.* Antinociceptive effect of astragalosides and its mechanism of action. Acta Pharmacol Sin 2001;22:809-12.
29. Li ZP, Cao Q. Effects of astragaloside IV on myocardial calcium transport and cardiac function in ischemic rats. Acta Pharmacol Sin 2002;23:898-904.
30. Lu S, Zhang J, Yang D. Effects of astragaloside in treating myocardial injury and myocardial sarco/Endoplasmic ca(2+)-ATPase of viral myocarditis mice. Zhongguo Zhong Xi Yi Jie He Za Zhi 1999;19:672-4.
31. Luo Y, Qin Z, Hong Z, Zhang X, Ding D, Fu JH, *et al.* Astragaloside IV protects against ischemic brain injury in a murine model of transient focal ischemia. Neurosci Lett 2004;363:218-23.
32. Tatsuguchi M, Seok HY, Callis TE, Thomson JM, Chen JF, Newman M, *et al.* Expression of microRNAs is dynamically regulated during cardiomyocyte hypertrophy. J Mol Cell Cardiol 2007;42:1137-41.
33. Manfè V, Biskup E, Rosbjerg A, Kamstrup M, Skov AG, Lerche CM, *et al.* MiR-122 regulates p53/Akt signalling and the chemotherapy-induced apoptosis in cutaneous T-cell lymphoma. PLoS One 2012;7:e29541.
34. Fornari F, Gramantieri L, Giovannini C, Veronese A, Ferracin M, Sabbioni S, *et al.* MiR-122/cyclin G1 interaction modulates p53 activity and affects doxorubicin sensitivity of human hepatocarcinoma cells. Cancer Res 2009;69:5761-7.
35. Huang S, Wang S, Bian C, Yang Z, Zhou H, Zeng Y, *et al.* Upregulation of miR-22 promotes osteogenic differentiation and inhibits adipogenic differentiation of human adipose tissue-derived mesenchymal stem cells by repressing HDAC6 protein expression. Stem Cells Dev 2012;21:2531-40.
36. Cox LS, Lane DP. Tumour suppressors, kinases and clamps: How p53 regulates the cell cycle in response to DNA damage. Bioessays 1995;17:501-8.
37. Haffner R, Oren M. Biochemical properties and biological effects of p53. Curr Opin Genet Dev 1995;5:84-90.
38. Ko LJ, Prives C. P53: Puzzle and paradigm. Genes Dev 1996;10:1054-72.
39. Hollstein M, Sidransky D, Vogelstein B, Harris CC. P53 mutations in human cancers. Science 1991;253:49-53.
40. Michalovitz D, Halevy O, Oren M. Conditional inhibition of transformation and of cell proliferation by a temperature-sensitive mutant of p53. Cell 1990;62:671-80.
41. Martinez J, Georgoff I, Martinez J, Levine AJ. Cellular localization and cell cycle regulation by a temperature-sensitive p53 protein. Genes Dev 1991;5:151-9.
42. Crook T, Marston NJ, Sara EA, Vousden KH. Transcriptional activation by p53 correlates with suppression of growth but not transformation. Cell 1994;79:817-27.
43. Komori T, Kishimoto T. Cbfa1 in bone development. Curr Opin Genet Dev 1998;8:494-9.
44. Enomoto H, Enomoto-Iwamoto M, Iwamoto M, Nomura S, Himeno M, Kitamura Y, *et al.* Cbfa1 is a positive regulatory factor in chondrocyte maturation. J Biol Chem 2000;275:8695-702.
45. Kundu M, Javed A, Jeon JP, Horner A, Shum L, Eckhaus M, *et al.* Cbfbeta interacts with runx2 and has a critical role in bone development. Nat Genet 2002;32:639-44.
46. Simeone A, Daga A, Calabi F. Expression of runt in the mouse embryo. Dev Dyn 1995;203:61-70.
47. Yamada C, Ozaki T, Ando K, Suenaga Y, Inoue K, Ito Y, *et al.* RUNX3 modulates DNA damage-mediated phosphorylation of tumor suppressor p53 at ser-15 and acts as a co-activator for p53. J Biol Chem 2010;285:16693-703.